BABEŞ-BOLYAI UNIVERSITY CLUJ-NAPOCA
FACULTY OF PHYSICS

Contributions to designing the optical properties of some plasmonic metamaterials

– Doctoral Thesis Summary –

Mircea Giloan

Scientific Advisor
Prof. Dr. Simion Aştilean

CLUJ-NAPOCA
2012

Contents

Keywords: Metamaterials, Negative index, Plasmons, Hybridization, Near-field enhancement, Enhanced optical transmission.

Introduction

Metamaterials are artificially engineered composite materials, made of densely packed micro– or nanostructured building blocks, displaying electromagnetic properties beyond those available in naturally occurring materials. Since the Greek word ‘meta’ means ‘beyond’ the term ‘metamaterials’ refers to ‘beyond conventional materials’. Due to metamaterials the classical subject of electromagnetism and optics have experienced a number of new discoveries and advances in research. In 1968 Victor Veselago theoretically investigated a material whose electric permittivity and magnetic permeability are simultaneously negative [1]. A number of unusual phenomena like negative refractive index and backward wave propagation were predicted by Veselago in this study. After more than 30 years of stagnation, due to the lack of experimental verification, negative refractive index materials (NIMs) have drawn attention of the scientific community when a negative permittivity medium was discovered by Sir Pendry in 1996 [2], followed by the discovery of negative permeability in 1999 by Sir Pendry et al. [3], and the first experimental realization of a NIM by Smith et al. in 2001 [4]. Negative index materials have lead to the development of superlenses capable of imaging at resolutions beyond the diffraction limit [5]. Another application of metamaterials is the gradient refractive index medium which allows an unprecedented control of light propagation [6]. Gradient index structures designed using the transformation optics approach [7] lead to new exciting applications like optical cloaks or optical illusions. In this thesis I have analyzed the optical properties of four different metamaterials made of metallic elements embedded in a dielectric matrix. The optical properties of these structures are based on plasmonic phenomena and two of them show a negative index of refraction one in the visible range and the other in the near infrared range.

1. Electromagnetic plane waves in isotropic and homogeneous media

This introductive chapter presents the basic theoretical concepts that describe the main characteristics of electromagnetic plane wave propagation in isotropic and homogeneous media. Maxwell’s equations along with the constitutive (material) equations and boundary conditions are fully describing the electromagnetic field in matter and at the interface between two different media. The concept of the refractive index is related to the wave equation which describes the propagation of an electromagnetic wave in terms of its electric

and magnetic fields. The refractive index is defined as $n = \sqrt{\varepsilon_r}\sqrt{\mu_r}$ thus n is positive for positive ε_r' and μ_r' and negative for negative ε_r' and μ_r'.

1.6 The $(\vec{E}, \vec{H}, \vec{k})$ trihedron

In a NIM the vectors $\vec{E}$, $\vec{H}$ and $\vec{k}$ form a left-handed system, hence NIMs are also called 'left-handed' materials (Fig. 1.1).

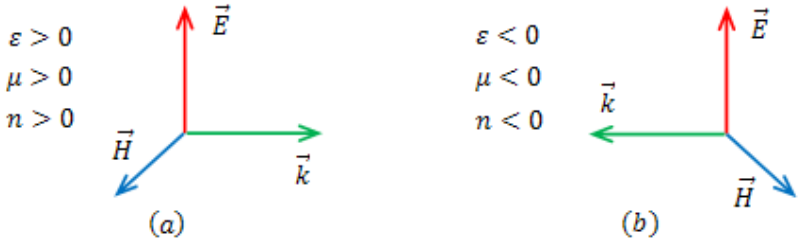

Figure 1.1 (a) 'Right-handed' trihedron $(\vec{E}, \vec{H}, \vec{k})$ in a positive index material (PIM); **(b)** 'Left-handed' trihedron $(\vec{E}, \vec{H}, \vec{k})$ in a NIM.

1.10 Electromagnetic wave refraction at the plane interface between two media

In a NIM the phase velocity is directed against the flow of energy. Also, at the interface between a positive and a negative index material, the refracted light is propagating on the same side of the normal as the incident light (Fig. 1.2).

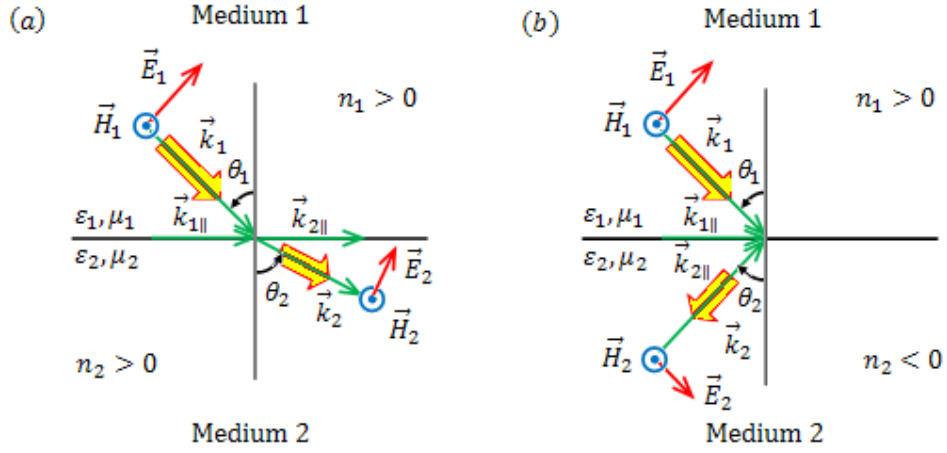

Figure 1.2 Light refraction at a PIM – PIM interface **(a)** and a PIM – NIM interface **(b)**.

2. Molding the electromagnetic properties of materials using metamaterials

The material properties are characterized by an electric permittivity and a magnetic permeability. Metamaterials are a new class of artificial composites which allow the molding of electric and magnetic response of the material by changing the geometry of the constituent elements. Advanced nanofabrication techniques allow the fabrication of materials with negative magnetic permeability and negative index of refraction in the optical range. The design of metamaterials with gradient magnetic permeability and electric permittivity leads to an unprecedented control of the electromagnetic field propagation and unusual applications like invisible cloaks. Negative index materials can also be used to design superlenses with resolution beyond the diffraction limit.

3. Models and methods for plasmonic metamaterials analysis

Two different approaches are used to fabricate negative index materials (NIMs). The first is using plasmonic resonant elements [8, 9] and the second is using plasmonic waveguides [10, 11]. The electromagnetic properties of plasmonic waveguides made NIMs are based on plasmonic modes of the constituent waveguides while the electromagnetic properties of plasmonic resonant elements made NIMs are based on resonant plasmonic states of the constituent elements. In this chapter is presented the theory of plasmonic modes for metal-dielectric interfaces with different geometries [12]. The spatial dispersion model, described in this chapter, explains the relationship between the local field response and the macroscopical behaviors for artificial metamaterials composed of periodic resonant structures [13]. The S-parameter retrieval method used to determine the constitutive parameters of an effective medium once the reflection and transmission coefficients are known [14], is also presented in the end of the chapter.

4. Experimental results and numerical simulations

In this chapter are presented experimental and theoretical results of analyzing the electromagnetic properties of two dielectric-metal structures.

4.1 Metallic nanocylinders structures

Two-photon micro fabrication is a standard technique used for producing metallic micro-and nanostructures. In fabrication process we used a Q-switched 1064 nm Nd-YAG laser as a source for two-photon reduction of silver ions from silver nitrate ($AgNO_3$) dissolved in a poly 4-styrensulfonic acid (PSS) solution [15, 16]. Vertical nanocylinders could be obtained because of the high spatial selectivity of the two-photon photo reduction process of silver positive ions (Ag^+). Typical fabricated nanocylinders diameter and length were approximately 200 nm and 5 μm respectively. The fabricated nanocylinders are embedded in a dielectric PSS polymer film of refractive index of 1.4 which is deposited on a microscope slide. The cylinders are arranged in a square lattice having the periodicity constant a=800 nm.

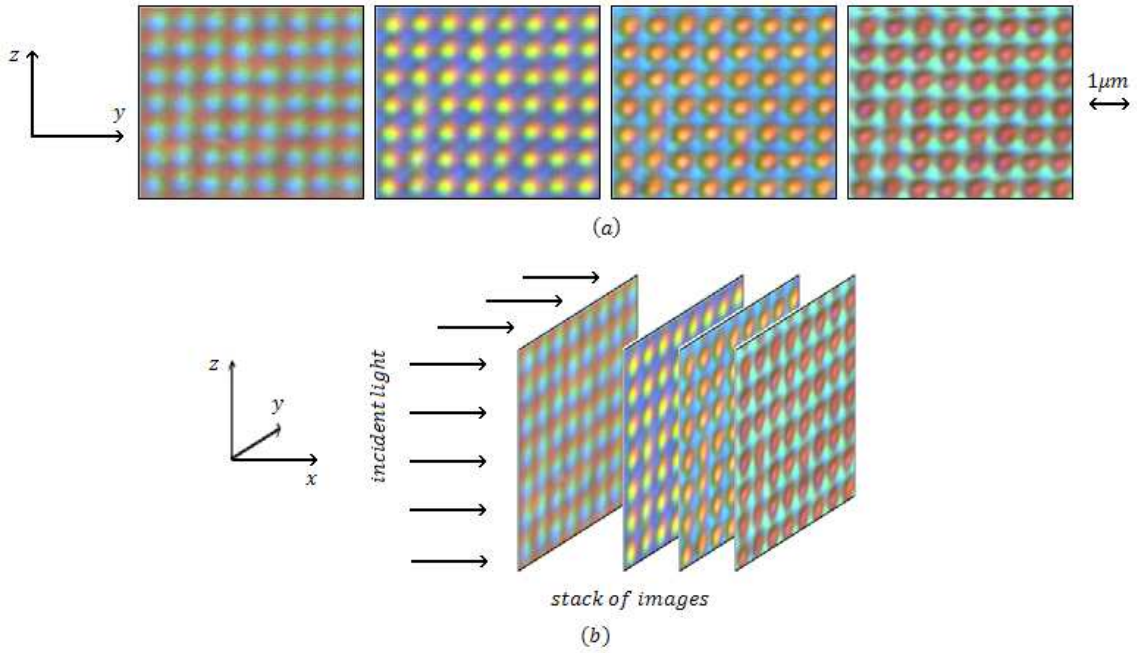

Figure 4.1 The light propagation along the cylinders was analyzed using a CCD camera.

The three-dimensional propagation of visible light along the cylinders has been characterized by wide field transmission microscopy with a high numerical aperture microscope objective (NA=1.4). Light propagation through the structure along OX axe was analyzed using a CCD camera and a visible - near infrared spectrometer. For different x values pictures of the structure in YOZ plane were captured (see figure 4.1(a)) and further assembled in a stack in the succession of increasing x which corresponds to the light propagation direction (see figure 4.1(b)). Cross sections through the resulting stack provide us useful information about the light intensity inside the structure along the propagation direction. Intensity distribution

along the cylinders and between cylinders for visible range wavelengths are presented in figure 4.2.

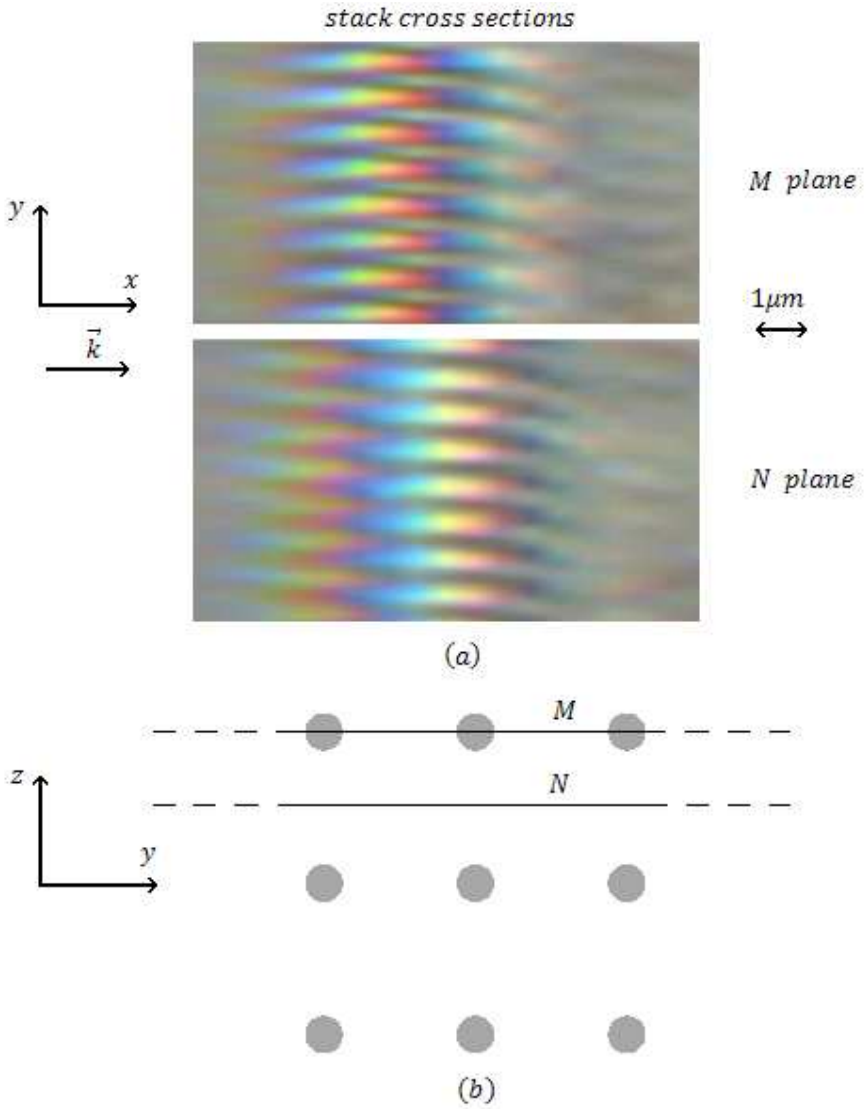

Figure 4.2 (a) Light distribution on plane M (up) crossing the cylinders, and plane N (down) placed between cylinders (see figure **(b)**).

The electromagnetic field distribution along the silver cylinders were computed using FDTD method. In the case of 5 μm long cylinders, simulation results, show two areas of near-field intensity enhancement along the cylinders surface for wavelengths ranging from 600 nm to 750 nm. When the length of the cylinders is reduced at 3 μm only one area of near-field intensity enhancement along the cylinders surface can be observed for wavelengths ranging from 600 nm to 750 nm. Figure 4.3 shows volume (V) versus field enhancement ($\Gamma = \mathbf{E}\cdot\mathbf{E}^*/\mathbf{E_0}\cdot\mathbf{E_0}^*$) variation for wavelength equal to 600 nm. We can see that the field enhancement

volume for the first zone of 5 μm long cylinders and for 3 μm long cylinders are approximately the same, hence the cylinders length has almost no influence upon near-field intensity enhancement [17].

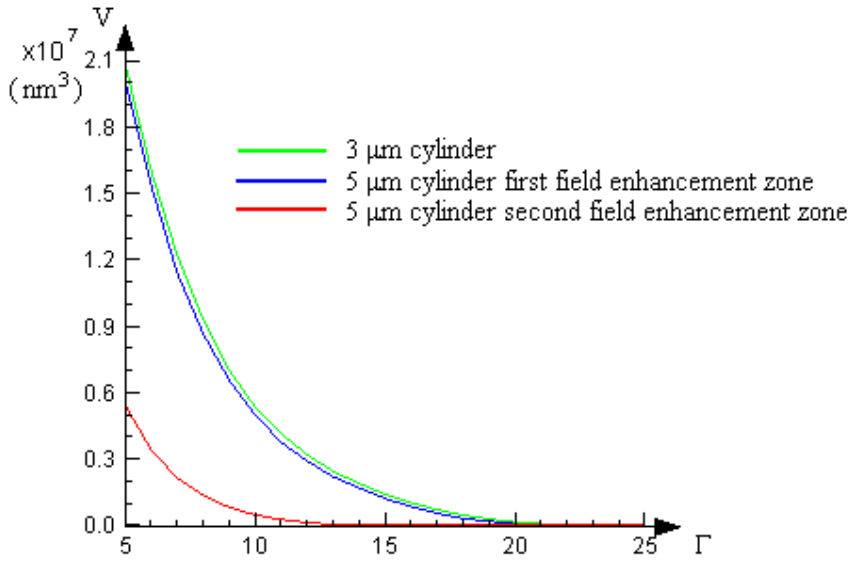

Figure 4.3 Volume of the enhanced fields around a cylinder (V) versus electromagnetic field enhancement (Γ). The wavelengths of incident light is λ = 600 nm.

4.2 Metallic films over colloidal particles structures

Two-dimensional colloidal crystals (CC) were prepared from polystyrene (pS) spheres (Polysciences) with a diameter of 450 nm. The CC were obtained by using a self-organization method often named drop-coating. It involves dispensing a drop of colloidal solution onto a hydrophilic glass surface, and allow the solvent (in our case water) to evaporate, leaving a close-packed hexagonal array of colloids on the substrate [18]. Silver films were deposited by means of vacuum thermal evaporation, and film thickness was monitored by a quartz crystal microbalance, to about 50 nm on all the samples discussed in this study.

The optical transmission and reflection measurements were performed on a Jasco V-530 spectrophotometer using unpolarized light. An opaque pierced screen was used as a mask to limit the spot diameter to about 2 mm^2. Computer simulations of the electromagnetic response of the structure are performed using a three-dimensional finite-difference time domain algorithm (FDTD) [19]. Figure 4.4 presents the experimental and simulated spectra

of transmittance (T), reflectance (R), and absorbance (A=1-T-R) for the analyzed structure, at normal incidence. The light is propagating from above the silver film and is exiting through the glass substrate.

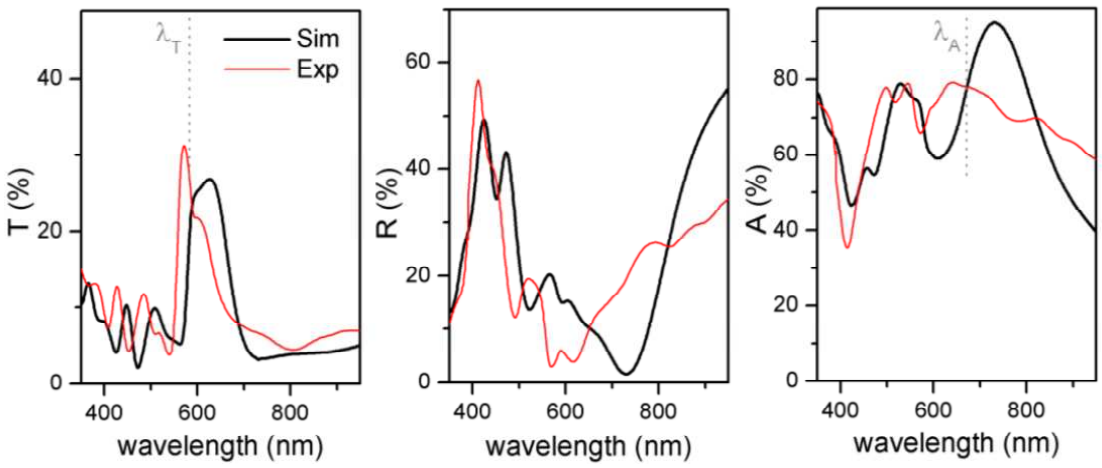

Figure 4.4 Comparison of simulated (thin red lines) and experimental (thick black lines) transmission (T), reflection (R), and absorption (A) spectra of silver film over colloidal crystal (AgFoCC).

Experimental measurements and computer simulations are in good agreement and show that strong absorption is present at wavelengths longer than the transmission maximum, different than what is usually observed in enhanced optical transmission (EOT) through optically thick film perforated with regular arrays of nanoholes [20, 21]. In order to explain the transmission and absorption spectra the component of the electric field intensity parallel to the propagation direction (E_x) was computed near the silver film deposited over the polystyrene spheres and analyzed for the wavelengths corresponding to the maximum values of transmission (λ_T) and absorption (λ_A). Figure 4.5 shows the real part of the E_x component of the electric field intensity for $\lambda_T = 580\,nm$ and $\lambda_A = 670\,nm$. Analyzing the field distribution one can identify a symmetric and an anti-symmetric plasmonic mode corresponding to the wavelength $\lambda_A = 670\,nm$ respectively $\lambda_T = 580\,nm$ [22, 23]. Figure 4.6 shows the electric charge distribution for these hybridized plasmonic modes [24].

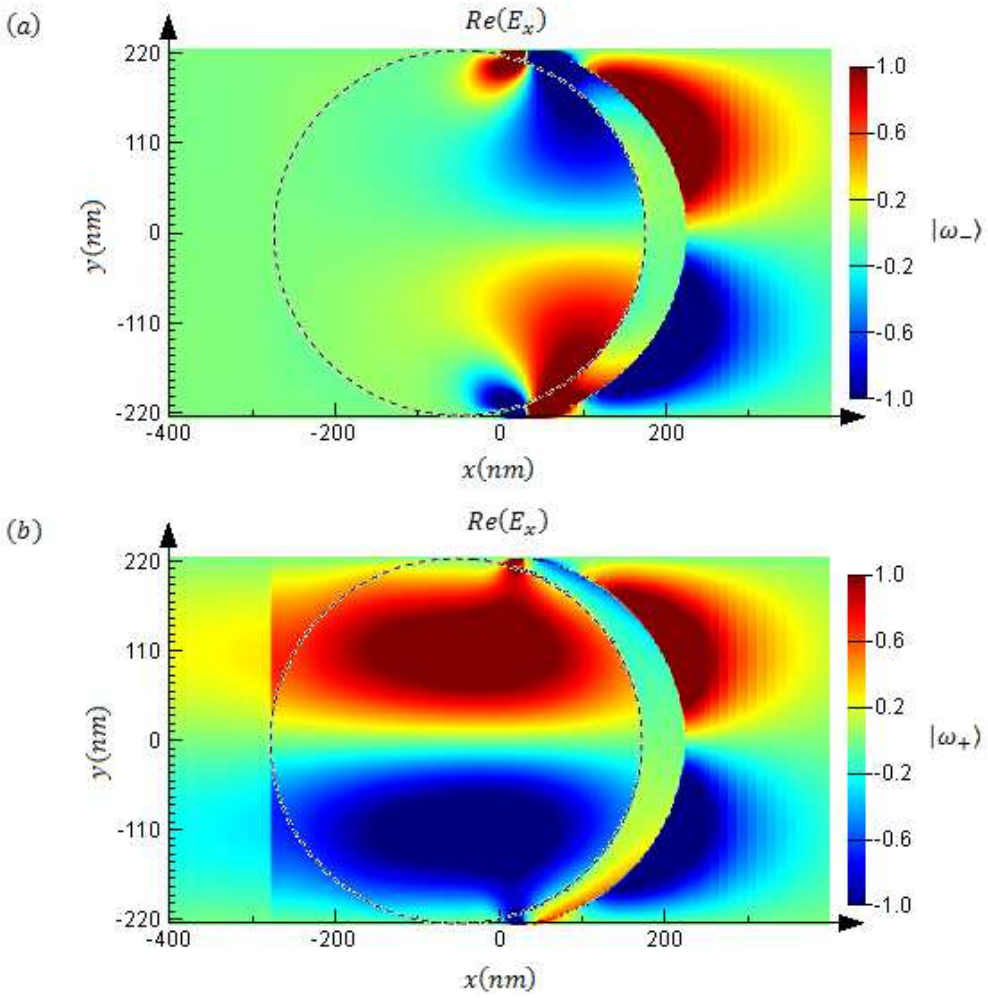

Figure 4.5 Distribution of the real part of E_x for $\lambda_A = 670\,nm$ **(a)** and $\lambda_T = 580\,nm$ **(b)** correspond to symmetric $|\omega_-\rangle$ and anti-symmetric $|\omega_+\rangle$ plasmonic modes respectively. The polarization of the incident light is parallel to OY axis.

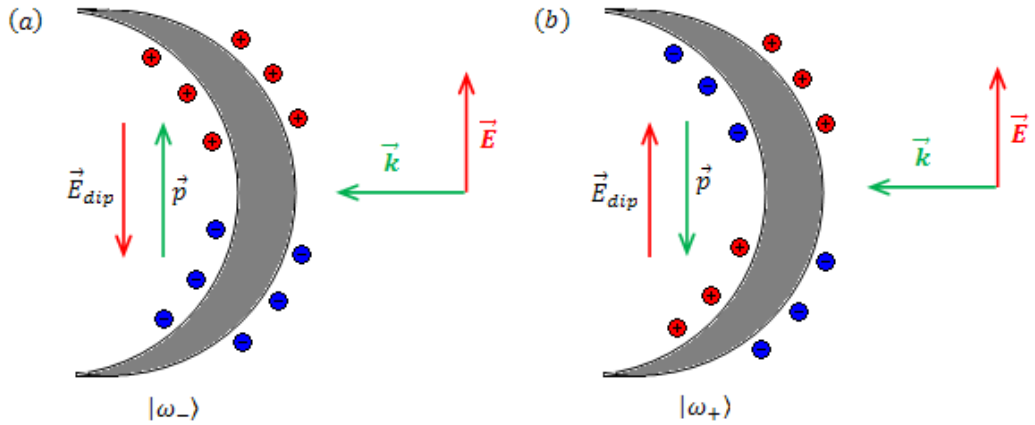

Figure 4.6 Electric charge distribution on the silver film surfaces for the symmetric $|\omega_-\rangle$ **(a)** and anti-symmetric $|\omega_+\rangle$ **(b)** plasmonic modes.

5. Resonant plasmonic metamaterials

In this chapter are presented two original theoretical results of negative index materials based on plasmonic resonant nano-elements.

5.2.2 Plasmonic metamaterials made of triangular nanoprisms in a hexagonal lattice

In this section we analyze theoretically the electromagnetic properties of a metamaterial slab made of gold triangular nanoprisms arranged in a hexagonal lattice. This structure is suitable for fabrication using self-assembly sphere lithography (SSL) technique [25]. Using different diameter polystyrene spheres combined with chemical etching technique one can adjust the dimension of the fabricated triangular nanoprisms as well as the lattice constant of the hexagonal lattice.

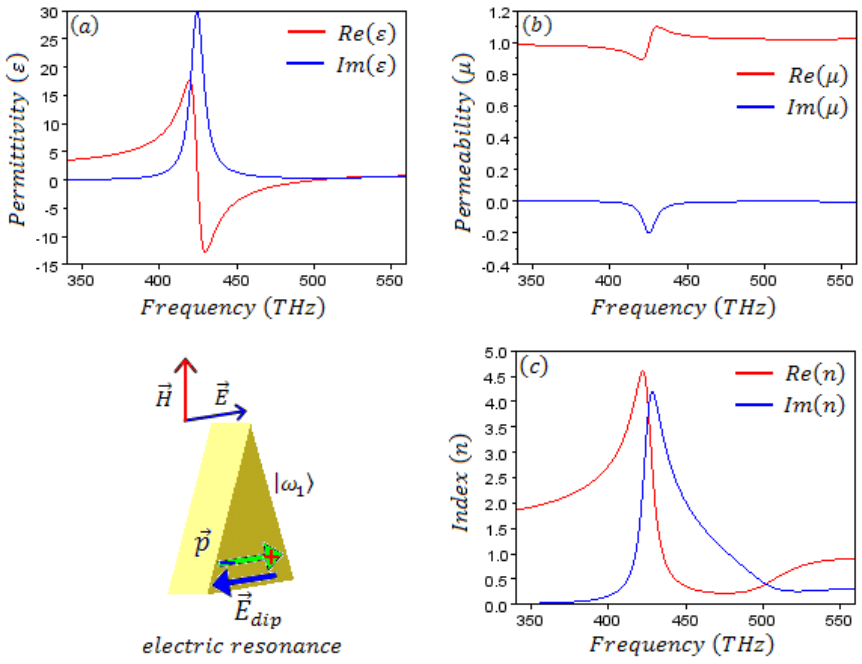

Figure 5.1 Constitutive parameters: permittivity **(a)**, permeability **(b)**, and refractive index **(c)**. Polarization of the incident light is parallel to one side of the triangular nanoprisms.

For nanoprisms dimensions and lattice constants in the range of hundreds of nanometers the structure presents reflection and transmission responses at optical frequencies due to the plasmonic resonances of the constituent nanoparticles. The geometrical dimensions of the simulated structure are the following: hexagonal lattice constant a=450 nm, triangular prisms side length L=165 nm, and prisms thickness h=30 nm. Following the retrieval process of the constitutive parameters, the real and imaginary parts of the relative permittivity and permeability are obtained as presented in figure 5.1. Analyzing the real and imaginary parts

of the relative permittivity, we can observe the presence of a typical electric resonance around the frequency of 426 THz.

5.2.3 Plasmonic metamaterials made of two overlapped layers of triangular nanoprisms in a hexagonal lattice

In order to achieve a magnetically active metamaterial we added an identical layer of nanoprisms. The resulting bi-layered metamaterial has a spacing of s=30 nm between layers.

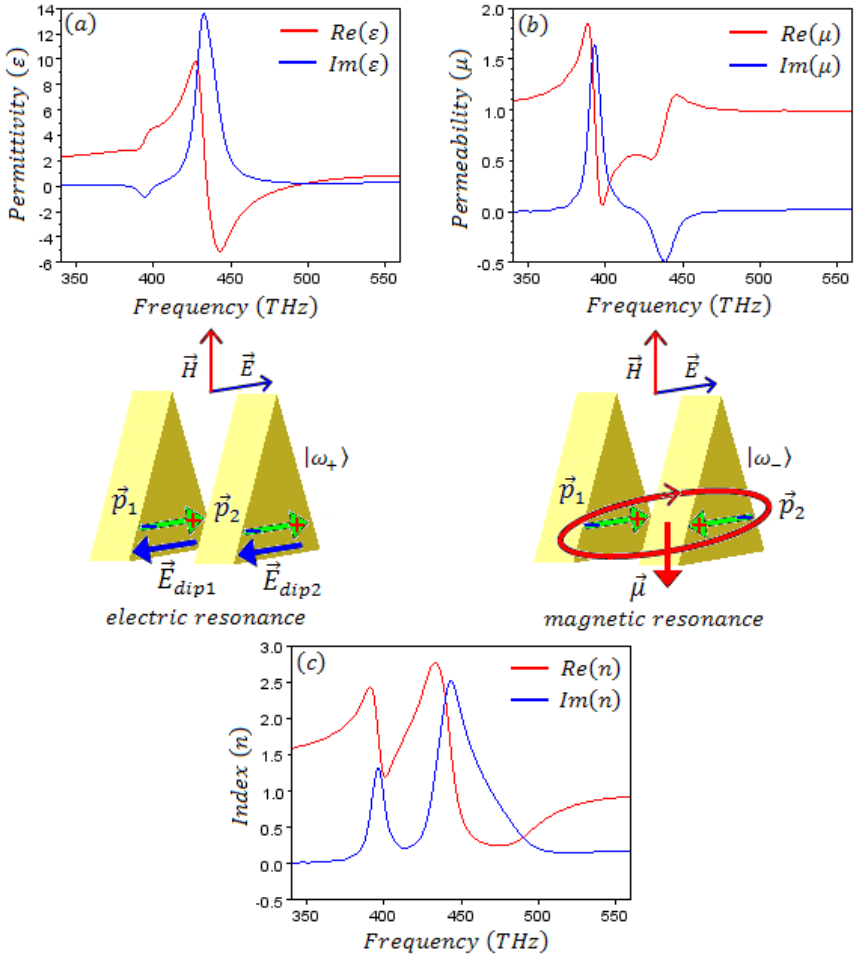

Figure 5.2 Material parameters: permittivity **(a)**, permeability **(b)**, and refractive index **(c)**.

The retrieved constitutive parameters: permittivity, permeability, and refractive index are presented in figure 5.2. The analyzed metamaterial slab made of two layers of overlapping equilateral triangular nanoprisms arranged in a hexagonal lattice, presents both a magnetic (f_-=397 THz) and an electric resonance (f_+=442 THz) corresponding to the anti-symmetric and symmetric hybridized plasmonic modes, respectively. The magnetic resonance exhibits

values going close to zero for the real part of the permeability, while the electric resonance exhibits negative values for the real part of the permittivity.

5.2.4 Plasmonic metamaterials made of two shifted layers of triangular nanoprisms in a hexagonal lattice

In order to design a metamaterial with a negative index of refraction we introduced a shift between layers (d_y) in the direction of the electric field polarization.

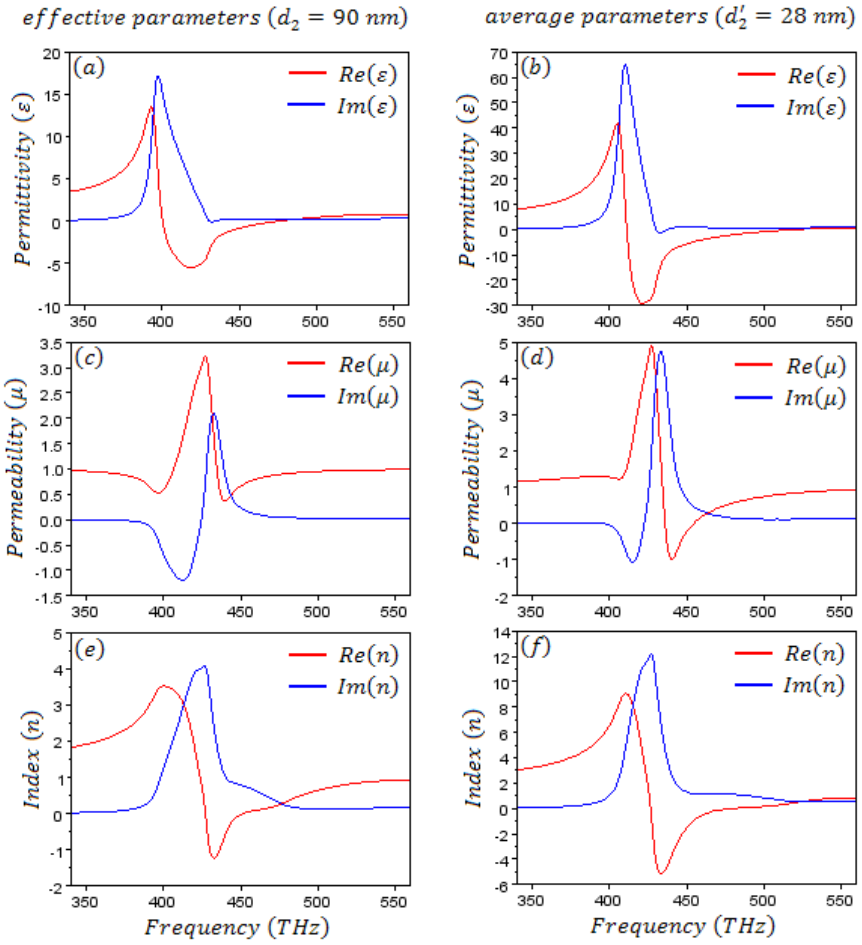

Figure 5.3 Effective constitutive parameters: permittivity **(a)**, permeability **(c)**, and refractive index **(e)**. Average constitutive parameters: permittivity **(b)**, permeability **(d)**, and refractive index **(e)**.

For a sufficiently large displacement d_y=120 nm, the hybridization scheme is slightly inverted with the symmetric mode at a lower frequency than the anti-symmetric mode and a negative refractive index is achieved at optical frequencies between 430 and 450 THz. Figure 5.3 shows the effective constitutive parameters for a metamaterial thickness of d_2=90 nm and also the average constitutive parameters for a thickness of d_2'=28 nm.

5.3 Polarization insensitive negative refractive index metamaterial

Hexagonal arrays of gold nanoelements with C_3 symmetry are studied as a metamaterial slab of reduced anisotropy. Tri-dimensional (3D) finite-difference time domain (FDTD) simulations are used to calculate the reflected and transmitted electromagnetic field for two waves normally incident to the slab with mutually perpendicular polarizations. S-parameter method is used to retrieve the constitutive parameters for each polarization. While dipolar plasmonic resonance in the case of one layer metamaterial slab leads only to negative values of permittivity, using two layers of asymmetric nanoelements leads to a negative refractive index metamaterial in the near infrared range (158-172 THz) as a result of hybridized plasmonic states inversion.

5.3.1 The structure of the constituent nano-elements of the studied metamaterials

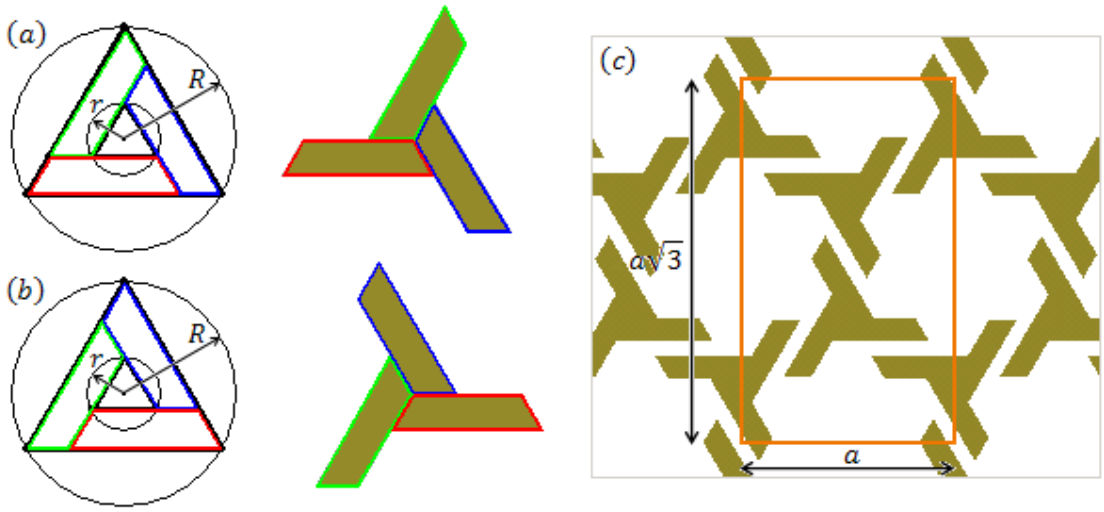

Figure 5.4 The asymetric resonant nanoelements **(a)** and **(b)**. Elementary cell used in simulations **(c)**.

The design of nanoelements is presented in Fig. 1(a) and (b). Three isosceles trapezoids, of which parallel sides are forming two equilateral triangles, can be defined in two ways, as shown in Fig. 5.4(a) and (b) (left), respectively. The constituent nanostructures of the studied metamaterials are obtained by translating these three trapezoids so that the common vertices of the trapezoids and the inner equilateral triangle are translated into the center of the triangle (see Fig. 5.4(a) and (b) right). In this way two different kinds of “meta-atoms” mutually asymmetric are created. The resulting “meta-atoms” can be dimensionally characterized

through the circumradii length of the inner and outer equilateral triangles, r and R respectively.

5.3.2 Symmetric and anti-symmetric hybridized plasmonic modes inversion

Figure 5.5 presents the transmission spectra for a single layer metamaterial (blue), a symmetric double layer metamaterial (green), and an asymmetric double layer metamaterial (red). Hybridized plasmonic modes inversion occurs in the case of asymmetric metamaterial.

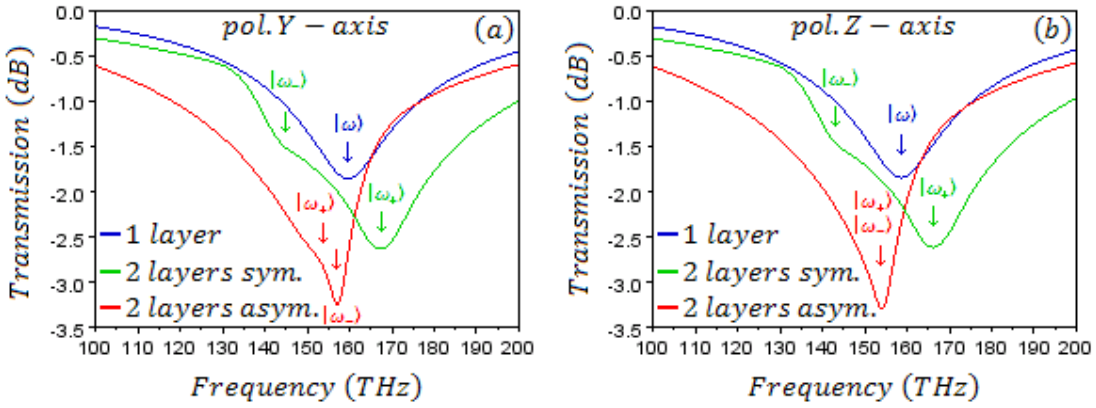

Figure 5.5 Hybridized plasmonic modes inversion occurs for a bi-layered asymmetric metamaterial for each polarization direction OY **(a)** and OZ **(b)**.

In our study we analyze theoretically the electromagnetic properties of three metamaterials, one single layered and two double layered slabs all of them having the hexagonal lattice constant a=450 nm. The constituent "meta-atoms" are made from gold with dimensions given by r=50 nm and R=150 nm, as mentioned in the previous section, and thickness h=30 nm. Reflected and transmitted light through the metamaterial slab at normal incidence are obtained by performing computer simulations using a three-dimensional (3D) finite-difference time domain algorithm (FDTD). We consider also a surrounding medium refractive index of n=1.5. In order to analyze the polarization dependence of the materials transmission two waves with mutually perpendicular polarizations are used.

5.3.3 Effective parameters of the studied metamaterials

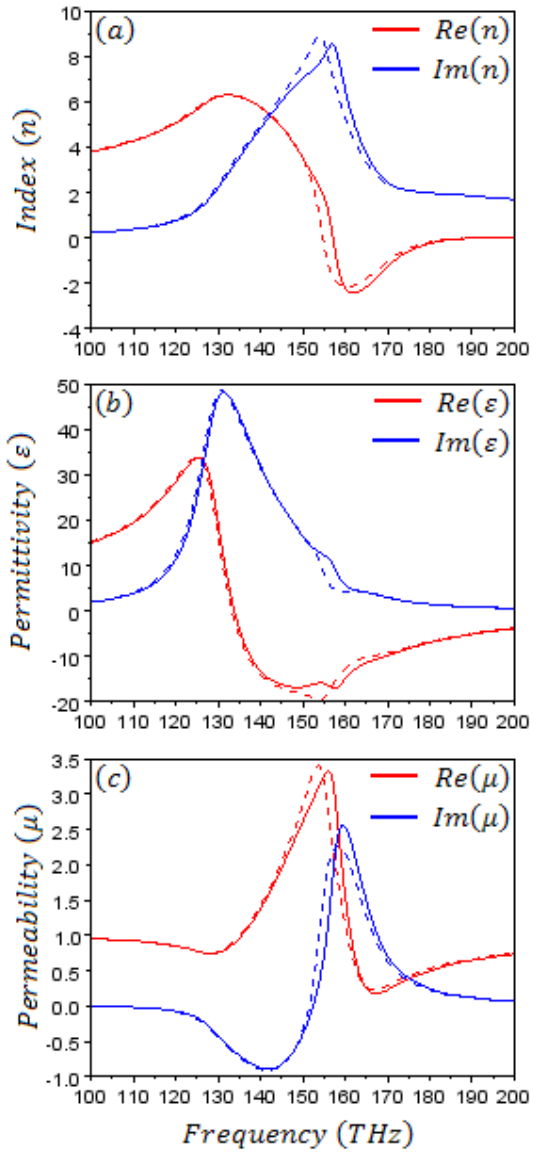

Figure 5.6 Effective constitutive parameters for the double layer asymmetric metamaterial. Refractive index **(a)**, electric permittivity **(b)**, magnetic permeability **(c)**.

The asymmetric double layered structure shows that the symmetric and anti-symmetric plasmonic modes frequencies can be equalized or even slightly inverted by controlling the interaction between the constituent nanostructures, as we saw in the previous section. Analyzing the real and imaginary part of the relative permittivity (Fig. 5.6(b)) and permeability (Fig. 5.6(c)) we can observe the electric and magnetic resonances around the same frequency f_{3el}= f_{3mag}=158 THz for both polarizations. Also a negative real part of the

refractive index (*n*') is obtained in the range of frequencies from 158 THz to 172 THz for both polarizations (Fig. 5.6(a)).

6. General conclusions and perspectives

1.a) Vertical silver nanocylinders have been fabricated by two-photon microfabrication technique. The three-dimensional propagation of visible light along and between the nanocylinders has been characterized by wide-field transmission microscopy. Transmission spectra were collected with a fiber coupled spectrometer and optical images were taken with a camera using an inverted microscope. Intensity enhancements occur along the nanocylinders surfaces for wavelengths in the visible range. Finite-difference time domain (FDTD) simulations are in good agreement with the experimental results. The electromagnetic field enhancement was evaluated, in order to analyze the suitability of the studied structures for sensing applications.

1.b) Metal films deposited over two-dimensional colloidal crystals (MFoCC) constitute a low-cost periodic structure with interesting photonic and plasmonic properties. It has previously been shown that this structure exhibits a behavior similar to the well-known Extraordinary Optical Transmission (EOT) of metallic hole arrays in planar films. Transmission and absorption spectra were explained by analyzing the near field distribution which shows the presence of two hybridized symmetric and anti-symmetric plasmonic modes.

2.a) Mono and bi-layered structure made of gold triangular nanoprisms in a hexagonal lattice were theoretically analyzed. A metamaterial slab made of one layer presents an electric resonance, leading to negative values of permittivity, due to the dipolar plasmonic resonance of the constituent nanoprisms. A metamaterial slab made of two layers, with no displacement between layers, presents both a magnetic and an electric resonance corresponding to the anti-symmetric and symmetric hybridized plasmonic modes, respectively. Introducing a shift between layers, in the direction of the electric field, we demonstrated that the coupling between the localized plasmons, on the surface of the prisms from different layers, can be controlled. For a sufficiently large displacement, the hybridization scheme is slightly inverted with the symmetric mode at a lower frequency than the anti-symmetric mode, and a negative refraction index is achieved at optical frequencies (430–450 THz).

2.b) In this work we studied, using tri-dimensional FDTD computer simulations, the electromagnetic properties of single and double layered metamaterials consisting of gold

nanoelements arranged in a hexagonal lattice. Asymmetric double layered metamaterial slab, with asymmetric nanostructures geometry in one layer with respect to the other, demonstrates that controlling the coupling between the localized plasmons, on the surface of the nanoelements from different layers, the hybridized plasmonic modes can be slightly inverted so that the symmetric mode appears at a lower frequency then the anti-symmetric mode. Consequently a negative refraction index is achieved at near infrared frequencies (158 - 172 THz). Due to the hexagonal lattice and to the 120^0 rotational symmetry (C_3) of the constituent nanoelements the electromagnetic parameters of the studied metamaterial are polarization insensitive.

Selected references

1. V.G. Veselago, "The Electrodynamics of Substances with Simultaneously Negative Values of ε and μ," Sov. Phys. Uspekhi. 10, 509-514 (1968).

2. J.B. Pendry, A.J. Holden, W.J. Stewart, and I. Youngs, "Extremely Low Frequency Plasmons in Metalic Meso Structures," Phys. Rev. Lett. 76, 4773-4776 (1996).

3. J.B. Pendry, A.J. Holden, D.J. Robbins, and W.J. Stewart, "Magnetism from Conductors, and Enhanced Non-Linear Phenomena," IEEE Trans. Microwave Theory Tech. 47, 2075 (1999).

4. R.A. Shelby, D.R. Smith, and S. Schultz, "Experimental Verification of a Negative Index of Refraction," Science 292, 77-79 (2001).

5. J.B. Pendry, "Negative refraction makes a perfect lens," Phys. Rev. Lett. 85, 3966-3969 (2000).

6. D.R. Smith, J.J. Mock, A.F. Starr, and D. Schurig, "Gradient index metamaterials", Phys. Rev. E 71, 036609 (2005).

7. J.B. Pendry, D. Schurig, and D.R. Smith, "Controlling Electromagnetic Field," Science 312, 1780-1782 (2006).

8. V. M. Shalaev, "Optical negative-index metamaterials," Nature Photon. 1, 41-48 (2007).

9. A. Alu, A. Salandrino, and N. Engheta, "Negative effective permeability and left-handed materials at optical frequencies," Opt. Express 14, 1557-1567 (2006).

10. J.A. Dionne, E. Verhagen, A. Polman, and H.A. Atwater, "Are negative index materials achievable with surface plasmon waveguides? A case study of three plasmonic geometries," Opt. Express, 23, 19001-19017 (2008).

11. E. Verhagen, R. de Waele, L. Kuipers, and A. Polman, "Three-Dimensional Negative Index of Refraction at Optical Frequencies by Coupling Plasmonic Waveguides," Phys. Rev. Lett. 105, 223901 (2010).

12. D. Sarid, and W. Challener, *Modern Introduction to Surface Plasmons: Theory, Mathematica Modeling, and Applications*, Cambridge University Press, 2010.

13. R. Liu, T.J. Cui, D. Huang, B. Zhao, and D.R. Smith, “Description and explanation of electromagnetic behaviors în artificial mtamaterials based on effective medium theory,” Phys. Rev. E, 76, 026606 (2007).

14. D.R. Smith, S. Schultz, P. Markos, and C.M. Soukoulis “Determination of effective permittivity and permeability of metamaterials from reflection and transmission coefficients,” Phys. Rev. B, Vol. 65, 195104, (2002).

15. I. Wang, M. Bouriau, P.L. Baldeck, C. Martineau and C. Andraud, “Three-dimensional microfabrication by two-photon initiated polymerization using a low-cost microlaser,” *Opt. Lett.*, 27, 1348-1350 (2002).

16. L. Vurth, P. Baldeck, O. Stephan and G. Vitrant, “Two-photon induced fabrication of gold microstructures în polystyrene sulfonate thin films using a ruthenium(II) dye as photoinitiator,” *Appl. Phys. Lett.*, 92, 171103 (2008).

17. **M. Giloan**, S. Zaiba, G. Vitrant, P. L. Baldeck and S. Astilean “Light transmission and local field enhancement în arrays of silver nanocylinders,” Opt. Comm., 284, 3629-3634 (2010).

18. N. D. Denkov, O. D. Velev, P. A. Kralchevsky, I. B. Ivanov, H. Yoshimura, and K. Nagayama, “Two-dimensional crystallization,”, Nature 361, 26 (1993).

19. Lumerical Solutions Inc., “FDTD Solutions Online Help,” http://www.lumerical.com.

20. T.W. Ebbesen, H.J. Lezec, H.F. Ghaemi, T. Thio, and P.A. Wolff, “Extraordinary optical transmission through sub-wavelength hole arrays”, Nature 391, 667 (1998).

21. H.F. Ghaemi, T. Thio, D.E. Grupp, T.W. Ebbesen, and H.J. Lezec, “Surface plasmons enhance optical transmission through subwavelength holes”, Phys. Rev. B 58, 6779 (1998).

22. H. Wang, D.W. Brandl, P. Nordlander and N.J. Halas “Plasmonic Nanostructures: Artificial Molecules,” Acc. Chem. Res. 40, 53-62, (2007).

23. N.J. Halas, S. Lal, W.-S. Chang, S. Link, and P. Nordlander, “Plasmons în Strongly Coupled Metallic Nanostructures”, Chem. Rev. 111, 3913–3961, (2011).

24. C. Farcau, **M. Giloan**, E. Vinteler and S. Astilean “Understanding plasmon resonances of metal-coated colloidal crystal monolayers,” Appl. Phys. B, article in press (2011) DOI 10.1007/s00340-011-4849-9.

25. W.A. Murray, S. Astilean, and W.L. Barnes, “Transition from localized surface plasmon resonance to extended surface plasmon-polariton as metallic nanoparticles merge to form a periodic hole array”, Phys. Rev. B 69, 165407 (2004).

26. **M. Giloan**, S. Astilean “Visible frequency range negative index metamaterial of hexagonal arrays of gold triangular nanoprisms,” Opt. Comm., article in press (2011) DOI: 10.1016/j.optcom.2011.11.093.

27. **M. Giloan**, S. Astilean “Designing polarization insensitive negative index metamaterial for operation în near infrared” Opt. Comm., article in press (2011) DOI: 10.1016/j.optcom.2011.12.096.

List of papers

1. **M. Giloan**, S. Astilean "Designing polarization insensitive negative index metamaterial for operation în near infrared" Opt. Comm., article in press (2011) DOI: 10.1016/j.optcom.2011.12.096.

2. **M. Giloan**, S. Astilean "Visible frequency range negative index metamaterial of hexagonal arrays of gold triangular nanoprisms," Opt. Comm., article in press (2011) DOI: 10.1016/j.optcom.2011.11.093.

3. C. Farcau, **M. Giloan**, E. Vinteler and S. Astilean "Understanding plasmon resonances of metal-coated colloidal crystal monolayers," Appl. Phys. B, article in press (2011) DOI 10.1007/s00340-011-4849-9.

4. **M. Giloan**, S. Zaiba, G. Vitrant, P. L. Baldeck and S. Astilean "Light transmission and local field enhancement în arrays of silver nanocylinders," Opt. Comm., 284, 3629-3634 (2010).

Acknowledgments

I would like to thank all the people who helped me and who have also contributed to this thesis. Many thanks go to:

- Prof. Simion Aştilean for giving me the opportunity to work in the exciting filed of optical metamaterials, for his mentorship, and for many stimulating discussions.
- Dr. Patrice L. Baldeck for his mentorship, and stimulating discussions during my work at Laboratoire de Spectrométrie Physique, CNRS UMR 5588, Grenoble University.
- Prof. Dana Dorohoi, Prof. Traian Petrişor, and Prof. Mihai Todica for kindly agreeing to referee this thesis.
- Prof. Vasile Chiş for offering me technical support to run my computer simulations.
- Mr. Gavril Săplăcan and Mr. Mircea Rusu for technical support.
- All my colleagues from the Nanobiophotonics Center of the Institute for Interdisciplinary Research in Bionanoscience for warm working atmosphere and their kind helps.
- Dr. Cosmin Farcău for stimulating discussions.
- Dr. Valentin Cânpean for technical support.
- Last, but not least, I would like to thank my parents and all of my friends. A special thank goes to my wife Ligia for her everlasting encouragement, support, and standing by me all the time.